Prediction of Polaronlike Vortices and a Dissociation Depinning Transition in Magnetic Superconductors: The Example of $ErNi_2B_2C$

Lev N. Bulaevskii and Shi-Zeng Lin

Theoretical Division, Los Alamos National Laboratory, Los Alamos, New Mexico 87545, USA
(Received 2 May 2012; published 9 July 2012)

In borocarbide $ErNi_2B_2C$, the phase transition to the commensurate spin density wave at 2.3 K leaves $1/20$ part of Ising-like Er spins practically free. Vortices polarize these spins nonuniformly and repolarize them when moving. At a low spin relaxation rate and at low bias currents, vortices carrying magnetic polarization clouds become polaronlike and their velocities are determined by the effective drag coefficient, which is significantly bigger than the Bardeen-Stephen (BS) one. As current increases, at a critical current J_c vortices release polarization clouds and the velocity as well as the voltage in the I-V characteristics jump to values corresponding to the BS drag coefficient. The nonuniform components of the magnetic field and magnetization drop as velocity increases, resulting in weaker polarization and discontinuous dynamic dissociation depinning transition. As current decreases, on the way back, vortices are retrapped by polarization clouds at the current $J_r < J_c$.

DOI: 10.1103/PhysRevLett.109.027001 PACS numbers: 74.25.Wx, 74.25.Ha, 74.70.Dd

The family of quaternary nickel borocarbides (RE)Ni_2B_2C (RE is rare earth magnetic ion) is an interesting class of crystals that exhibit both superconductivity and magnetic order at low temperatures [1–3]. A number of the crystals in that family develop antiferromagnetic order below the Néel temperature T_N below the superconducting critical temperature T_c. It has been recognized some time ago that superconductivity coexists quite peacefully with the antiferromagnetic order, as the spatial periodicity of magnetic moments is well below the superconducting correlation length. In contrast, the ferromagnetic order, antagonistic to the Cooper pairing, leads to dramatic changes in both magnetic and superconducting orders in the coexistence phase; for a review, see Ref. [4]. That is why interest in the compound $ErNi_2B_2C$ with $T_c = 11$ K and $T_N = 6$ K peaked when it was realized that below the phase transition from an incommensurate spin density wave (SDW) to a commensurate SDW at $T^* = 2.3$ K the phase with weak ferromagnetic ordering may emerge [5,6]. From neutron scattering data, it was concluded that in $ErNi_2B_2C$ below T_N the incommensurate SDW develops with effective Ising spins oriented along the a axis and with the wave vector $Q = 0.5526b^*$, where $b^* = 2\pi/b$ and b is the lattice period along the b axis [7,8]. At T^*, the transition to the commensurate phase with $Q = 0.55b^*$ leaves one out of 20 spins free of the SDW molecular field. These Er spins with the magnetic moment $\mu = 7.8\mu_B$ are easily polarizable by the magnetic field along the a direction. The spin magnetization in the magnetic field $H = 2000$ G in the temperature interval 2–4 K follows $M_{\mathrm{sp}}/H \approx \mu M_s/(k_B T)$, where $M_s \approx 56$ G; see Fig. 4 in Ref. [6]. This value, $M_s = \mu n$, corresponds to magnetization when all "free" spins with the concentration n order ferromagnetically. The same value M_s was obtained by extrapolation of the magnetization at temperature 2 K in fields $H > 1500$ G to $H \to 0$ [9]. Note that the Hall probe measurements below T^* without an applied field found a magnetic internal field much lower than M_s and no spontaneous vortex lattice was seen [10]. The high polarizability of the spin system in $ErNi_2B_2C$ is a key point for our following discussion.

As hope to observe remarkable consequences of a weak ferromagnetic phase coexisting with superconductivity waned, a few puzzles on $ErNi_2B_2C$ behavior at low temperatures remained. First, it was discovered by measuring the hysteresis in the M-H loops and transport measurements that a new pinning mechanism develops below T^* for which the critical current increases as temperature lowers [9,11]. Second, neutron scattering data in applied magnetic field $\mathbf{H}$ close to $\mathbf{H} \parallel \mathbf{c}$ have shown that vortices deviate randomly from the direction of the magnetic field inside the crystal [12]. The vortex deviations increase proportionally to $1/T$ as temperature drops from 4 to 1.6 K and is nearly independent of the magnetic field in contrast to the usual behavior when the effect of disorder drops with the field. So far, no explanation of the surprising temperature and field dependence of the critical current and disorder has been offered.

To explain these data, we propose a new mechanism of the pinning formation of polaronlike vortices dressed by the polarization cloud of the magnetic moments. The polaronic mechanism is inherent to all magnetic superconductors but it is best pronounced when the magnetic system is highly polarizable, as in the case of $ErNi_2B_2C$ below 4 K. To clarify this mechanism, we recall that the magnetic field is nonuniform within the vortex lattice, being strongest near the vortex cores. Consequently, the polarization of the magnetic moments is also nonuniform. When vortices move, they should repolarize the magnetic system; otherwise, they would lose the energy gained by polarization (the Zeeman energy). The process of repolarization depends on the dynamics of the magnetic system. In the following, we consider the relaxation dynamics of free spins in $ErNi_2B_2C$. The repolarization process is controlled by the relaxation time τ which should be compared with the characteristic time a/v needed to shift the vortex lattice moving with the velocity v by the vortex lattice period $a = (\Phi_0/B)^{1/2}$ (Φ_0 is the flux quantum, and B is the magnetic induction). For $\tau \gg a/v$, the magnetic moments strongly slow down the vortex motion. At some critical velocity and critical current, the vortices are stripped off the polarization clouds. The corresponding jump in velocity is strongly pronounced for large τ's. As current decreases, the vortices become retrapped again at the current $J_r < J_c$. Since the voltage $V \propto v$, the I-V characteristics show hysteresis. The physics here is similar to that of a polaron with vortices playing the role of electrons and the magnetic polarization in place of phonons [13].

The $ErNi_2B_2C$ crystals have orthorhombic structure below T_N with domains where a and b axes change by 90° in neighboring domains. We consider first a clean single-domain crystal and later will discuss the effect of domain walls. We consider the vortex lattice induced by applied magnetic field $\mathbf{H}$ tilted by the angle θ with respect to the crystal c axis. We choose the z axis along the direction of the vortex lines at rest and the x axis in the ac plane; see Fig. 1. The vortex line deviates from the applied field $\mathbf{H}$ due to the magnetic moments [12]. In the static situation, the direction of the vortex lines is determined by the effective field $\mathbf{H} + 4\pi\bar{\mathbf{M}}$. Here, $\bar{\mathbf{M}}$ is the spatial average of the magnetization. We denote by α the angle between

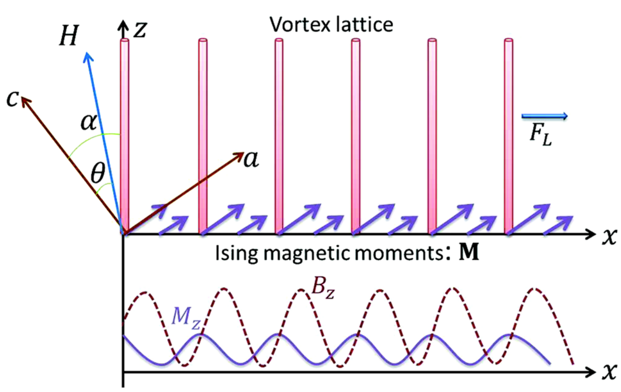

FIG. 1 (color online). Schematic view of the vortex lattice in the presence of free Ising magnetic moments along the a axis. The vortex lattice is tilted from the applied magnetic fields in the ac plane due to the polarization of the magnetic moments. The vertical columns show the vortex cores. The polarized magnetic moments are nonuniform in space due to the spatial modulation of the vortex lattice magnetic field. Due to the Lorentz force F_L, vortices move along the x axis. In the moving lattice, there is a phase shift between the magnetic induction (dashed line) associated with the vortex lattice and the magnetization (solid line) caused by the retardation in the response of the magnetic moments to the vortex magnetic field.

the vortex lines and the c axis. The deviation of the vortex lines from the applied magnetic field was also discussed in Ref. [14] in the case of the spontaneous ferromagnetic order of the magnetic moments.

In the London approximation, the magnetic field of the vortex lattice inside the crystal is ($\mathbf{r} = x, y$)

$$B_z(\mathbf{r}) = \bar{B}_z \sum_{\mathbf{G}} \frac{\cos(\mathbf{G}\cdot\mathbf{r})}{\lambda^2\mathbf{G}^2 + 1}, \quad (1)$$

where $\mathbf{G}$ are reciprocal vectors of the square lattice, λ is the superconducting penetration length renormalized by the magnetic moments, and $\bar{B}$ is the averaged magnetic induction. Here, we ignore anisotropy of the penetration length. As revealed by neutron scattering, vortices form a square lattice in $ErNi_2B_2C$ [12].

In the Lagrangian, the interaction between the vortex lines at $\mathbf{R}_i = (x_i, y_i)$ and the magnetic moments is determined by the term

$$\mathcal{L}_{\text{int}}\{\mathbf{R}_i, \mathbf{M}\} = -\int dt \int d\mathbf{r} B_z(\mathbf{R}_i - \mathbf{r}, t) M_z(\mathbf{r}, t), \quad (2)$$

where we describe the magnetic moments in the continuous approximation via the magnetization $M_z(\mathbf{r}, t)$, because distance between free spins, 35 Å [8], is much smaller than the London penetration length λ, about 500 Å [12]. We ignore the pair breaking effect [15] of the magnetic moments because they suppress Cooper pairing uniformly as distance between free spins is much smaller than the coherence length, and thus moments do not introduce pinning. We also neglect the effect of disorder in crystal lattice. The equation of motion for the vortex lines is

$$\eta \frac{\partial \mathbf{R}_i}{\partial t} = -\frac{\partial \mathcal{L}_{\text{vv}}\{\mathbf{R}_i, \mathbf{R}_j\}}{\partial \mathbf{R}_i} - \frac{\partial \mathcal{L}_{\text{int}}\{\mathbf{R}_i, \mathbf{M}\}}{\partial \mathbf{R}_i} + \mathbf{F}_L, \quad (3)$$

where η is the Bardeen-Stephen drag coefficient, $\mathcal{L}_{\text{vv}}\{\mathbf{R}_i, \mathbf{R}_j\}$ is the vortex-vortex interaction, the next term describes the force acting on the vortex line $\mathbf{R}_i$ from the magnetic moments, and $F_L = \Phi_0 J/c$ is the Lorentz force due to the bias current J. The force due to the magnetic moments is the same for all lines, and the vortex lattice moves as a whole. The motion of the vortex lattice center of mass, $u(t)$, along the x axis is described by the equation

$$\eta \frac{\partial u}{\partial t} = \frac{\partial}{\partial u}\left[\int d\mathbf{r} B_z(x+u, y, t) M_z(\mathbf{r}, t)\right] + F_L. \quad (4)$$

Using the linear response approach to relate the magnetization with the magnetic field, we obtain

$$\eta \frac{\partial u}{\partial t} = \frac{\partial}{\partial u} \int d\mathbf{r} d\mathbf{r}' B_z(x+u, y, t) \times \int_0^t dt' \chi_{zz}(\mathbf{r}-\mathbf{r}', t-t') B_z(\mathbf{r}', t') + F_L. \quad (5)$$

Here, $\chi_{zz}(\mathbf{r}, t)$ is the dynamic susceptibility of the magnetic moments. The vortex lattice moves with a constant velocity, $u = vt$, in the steady state $t \gg \tau$. Integrating over coordinates and time, we obtain

$$\eta v = \sum_{\mathbf{G}} \frac{\chi_{zz}(\mathbf{G}, \mathbf{v}\cdot\mathbf{G})}{(\lambda^2\mathbf{G}^2 + 1)^2} + F_L, \qquad (6)$$

where $\chi_{zz}(\mathbf{k}, \omega)$ is the dynamic magnetic susceptibility in the Fourier representation. We see that the magnetic moments strongly affect the vortex motion if (a) the resonance condition $\mathbf{v}\cdot\mathbf{G} = \Omega(\mathbf{G})$ is fulfilled, where $\Omega(\mathbf{k})$ is the frequency of magnetic excitations with the momentum $\mathbf{k}$, and $\Omega(\mathbf{k}) \gg \Gamma(\mathbf{k})$, where $\Gamma(\mathbf{k})$ is the relaxation rate of excitation, and (b) the dynamics of the magnetic system is dominated by slow relaxation, $\Omega(\mathbf{k}) \lesssim \Gamma(\mathbf{k})$, favoring the formation of the polaron. In the former case, discussed in Ref. [16], the magnetic moments renormalize the vortex viscosity at high velocities when the alternating magnetic field of vortices is able to excite magnons. Here, we consider the latter case of free moments described by the relaxation dynamics with $\chi_{zz}(\mathbf{k}, \omega)$ given by

$$\chi_{zz}(\mathbf{k}, \omega) = \chi \sin^2\alpha \frac{1}{1 - i\omega\tau}, \qquad \chi = \frac{\mu M_s}{k_B T} \qquad (7)$$

at temperatures T below 4 K for $ErNi_2B_2C$ (the effect of ordered spins will be discussed below).

We introduce dimensionless quantities by expressing t in units of τ and u in units $G_0^{-1} = a/(2\pi)$. In the summation over G_y in Eq. (6), we account only for the dominant term with $G_y = 0$. For $G_0\lambda \gg 1$, we find an equation for the dimensionless vortex velocity

$$\tilde{\eta} v = F(v) + \tilde{F}_L,$$
$$F(v) = -v[\pi^2/3 + v^2 - \pi v \coth(\pi/v)], \qquad (8)$$

where we introduced the dimensionless parameters

$$\tilde{\eta} = \frac{4\pi^2\eta\lambda^4}{\chi\Phi_0^2\tau\sin^2\alpha}, \qquad \tilde{F}_L = \frac{4\pi^2 G_0\lambda^4 J}{\chi c \Phi_0 \sin^2\alpha}. \qquad (9)$$

The asymptotic behavior of $F(v)$ is $F(v) \approx -v$ at $v \ll 1$ and $F(v) \approx -\pi^4/(45v)$ at $v \gg 1$. The electric field due to the motion of the vortex lattice is given by $E = Bv/c$, and we obtain the I-V curves from Eq. (8), as depicted in Fig. 2. As v increases, the v-J curve changes from a weak current dependence $v = \tilde{F}_L/(1 + \tilde{\eta})$ to a stronger and usual Bardeen-Stephen behavior $v = \tilde{F}_L/\tilde{\eta}$. In Fig. 2 at $\tilde{\eta} = 0.1$, the I-V curve is hysteretic. Upon ramping up the bias current, the system jumps to the usual Bardeen-Stephen (BS) Ohmic curve at a current J_c, where the electric field increases discontinuously by the factor $1/\tilde{\eta}$ at $\tilde{\eta} \ll 1$. The jump, identified experimentally as the depinning transition, is caused by the dissociation of the vortex-magnon polaron. It is very similar to the dissociation of the usual electron-phonon polaron in high electric fields as described theoretically [17] and confirmed experimentally in metal oxides [18]. Upon decreasing the current, the vortices are retrapped by the polarization clouds at a threshold current J_r and the vortex lattice moves with a significantly enhanced viscosity at lower currents.

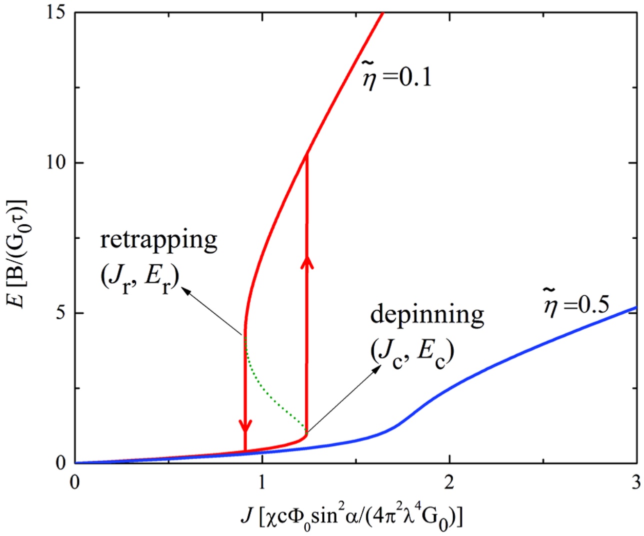

FIG. 2 (color online). Calculated I-V curves for $\tilde{\eta} = 0.1$ and $\tilde{\eta} = 0.5$. For $\tilde{\eta} = 0.1$, the system shows hysteresis in the I-V curve, while, for $\tilde{\eta} = 0.5$, no hysteresis is present. The green dotted line denotes the unstable solution.

The critical current J_c and retrapping current J_r follow from the equation for the velocity $\tilde{\eta} - dF(v)/dv = 0$. The maximum of $dF(v)/dv$ is 0.297; thus, hysteresis exists for $\tilde{\eta} < 0.297$. The calculated J_c, J_r, and corresponding electric fields are shown in Fig. 3. At small $\tilde{\eta}$, the critical current is

$$J_c \approx 0.03 \frac{\chi c \Phi_0 \sin^2\alpha}{G_0\lambda^4}. \qquad (10)$$

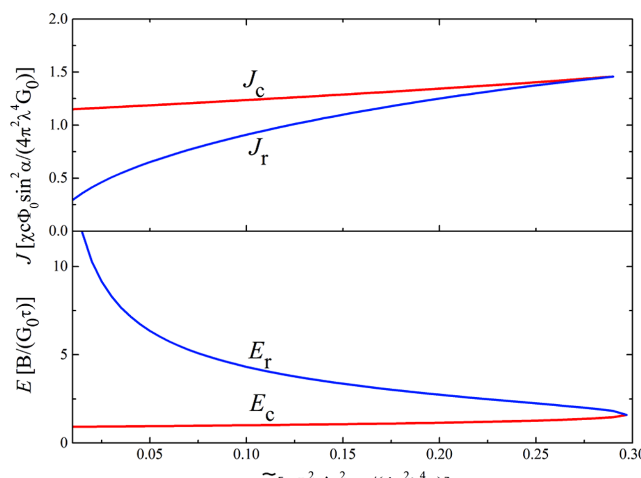

FIG. 3 (color online). Dependence of the critical current J_c and retrapping current J_r, and corresponding electric fields E_c and E_r on $\tilde{\eta}$.

J_c decreases with temperature as $J_c \sim 1/T$ and decreases with the magnetic field as $J_c \sim 1/\sqrt{B}$.

We note that above T^*, in the incommensurate SDW, some spins experience a quite weak SDW molecular field. Thus, they are polarized by vortices and exhibit the polaronic effect and pinning. This explains the increase of pinning in $ErNi_2B_2C$ as T decreases below T_N (see Ref. [9]), as well as pinning in the holmium borocarbide below T_N [19].

Let us consider the origin of the jumps at J_c and J_r. The dependence of the magnetization on the velocity of the moving vortices is

$$M_z(\mathbf{r}, \nu, t) = \chi \bar{B} \sin^2\alpha \sum_{\mathbf{G}} \frac{\cos[\mathbf{G}\cdot\mathbf{r} - \beta(\nu)]}{(\lambda^2\mathbf{G}^2 + 1)[1 + (G_x \nu\tau)^2]^{3/2}} \quad (11)$$

with $\tan(\beta) = G_x \nu\tau$. The nonuniform component of the magnetization and thus the polarization effect decrease with velocity. On the other hand, the retardation between the magnetic field and the magnetization, as described by the phase shift $\beta(\nu)$, increases with the velocity. This positive feedback and the increase of retardation with velocity ensure discontinuous transitions at J_c and J_r.

Strong pinning due to the polaron mechanism requires the small parameter $\tilde{\eta}$. It is expressed via τ as $\tilde{\eta} \approx 10^{-11}$ s$/(\tau \sin^2\alpha)$, where we have used the BS drag coefficient $\eta_{BS} = \Phi_0^2/(2\pi\xi^2 c^2 \rho_n)$ with the coherence length $\xi \approx 13$ nm [12] and the normal resistivity $\rho_n = 5\ \mu\Omega \cdot$ cm at T_c [20]. The relaxation time τ in $ErNi_2B_2C$ is long because the dynamics of the majority of spins is strongly suppressed by the formation of the SDW molecular field, as was found by the Mössbauer measurements [21]. The relaxation time drops very fast below 10 K and reaches the value $\tau \approx 5 \times 10^{-10}$ s at $T = 5$ K, but data at lower temperatures were not reported. Thus, the only information we have so far is $\tilde{\eta} < 0.02/\sin^2\alpha$.

The critical current for $ErNi_2B_2C$ reported in Ref. [9] for $B = 0.1$ T, $T = 2$ K is about 250 A/cm^2. Equation (10) gives such a current value at $\alpha = 2.5°$. In experiment, the applied magnetic field was close to the c axis, but the precise angle θ was not reported [9]. The estimate of the order of 1° is reasonable, but quantitative comparison is not convincing, as we do not know τ and thus $\tilde{\eta}$ below 2.3 K. Hence, the real check of the polaronic mechanism should be by measuring the I-V characteristics. We predict hysteretic behavior in $ErNi_2B_2C$ and strong dependence of voltage and of the critical current on the angle θ, at least for $\theta \gg 0.15$. Note that the critical current reaches values as high as 10^6 A/cm^2 at high angles at $T = 1$ K and $B = 0.1$ T.

The effect of ordered spins on the vortex motion is similar to that described in Ref. [16] for an antiferromagnet. When the Cherenkov condition $\mathbf{v}\cdot\mathbf{G} \geq \Omega(\mathbf{G})$ is met, the excitation of the magnons results in an enhanced viscosity η. This occurs at high velocities, due to a gap in the magnon spectrum, and thus at high currents $J > J_c$, leading to a voltage drop in comparison with the BS result.

Let us discuss now the effect of disorder on the vortex lines' direction observed in magnetic fields tilted with respect to the c axis [12]. Due to the domain structure, the Ising spins are polarized only in the half domains where the vortex lines follow the direction of the effective field $\mathbf{H} + 4\pi\mathbf{M}$, while in others they are along $\mathbf{H}$. The random change of the angle of the vortex directions with respect to the average angle is $2\pi M/B = 2\pi\chi \sin\alpha$. It increases as $1/T$, when T drops, in agreement with the results of Ref. [12] and the data for M_{sp}/H mentioned above. When vortices cross a domain wall between domains with different magnetization, they need to repolarize the magnetic moments at currents below the critical one. This additionally slows the vortex motion, but such an effect is smaller than that accounted for previously because the domain size is much bigger than the distance between the magnetic moments. The domain walls also cause the pinning of vortices, as seen in Bitter decoration patterns [22]. Importantly, for a nonzero θ, a small part of the vortices experiences domain wall pinning and this part drops with θ. In contrast, the polarization effect increases with θ, and this helps to separate the domain wall pinning from the polarization one.

In conclusion, vortices in magnetic superconductors polarize magnetic moments and become dressed and polaronlike. At low currents and long spin relaxation time, the nonuniform polarization induced by vortices slows their motion at currents for which pinning by the crystal lattice disorder becomes ineffective. As the current increases above the critical one, the vortices release the nonuniform part of the polarization and the velocity as well as the voltage in the I-V characteristics jump to much higher values. At decreasing current, vortices are retrapped by polarized magnetic moments at the retrapping current, which is smaller than the critical one. The results of such a polaronic mechanism are in qualitative agreement with the experimental data [9,12], but measurements of the I-V characteristics are needed to establish the quantitative agreement and confirm the validity of such a model for Er borocarbide. The polaronic mechanism should also be at play in Gd and Tb borocarbide superconductors in the commensurate SDW phase. It may be present in Tm borocarbide above T_N and in cuprate superconductors $(RE)Ba_2Cu_3O_7$, where magnetic RE ions positioned between superconducting layers interact weakly with superconducting electrons and order at very low Néel temperatures of the order 1 K [23].

The authors would like to thank P. Canfield, C. Batista, V. Kogan, D. Smith, A. Saxena, and B. Maiorov for helpful discussions. This publication was made possible by funding from the Los Alamos Laboratory Directed Research and Development Program, Project No. 20110138ER.

[1] P.C. Canfield, P.L. Gammel, and D.J. Bishop, Phys. Today **51**, No. 10, 40 (1998).
[2] S.L. Bud'ko and P.C. Canfield, C.R. Physique **7**, 56 (2006).
[3] L.C. Gupta, Adv. Phys. **55**, 691 (2006).
[4] L.N. Bulaevskii, A.I. Buzdin, M.L. Kulic, and S.V. Panjukov, Adv. Phys. **34**, 175 (1985).
[5] B.K. Cho, P.C. Canfield, L.L. Miller, D.C. Johnston, W.P. Beyermann, and A. Yatskar, Phys. Rev. B **52**, 3684 (1995).
[6] P. Canfield, S. Bud'ko, and B. Cho, Physica (Amsterdam) **262C**, 249 (1996).
[7] S.M. Choi, J.W. Lynn, D. Lopez, P.L. Gammel, P.C. Canfield, and S.L. Bud'ko, Phys. Rev. Lett. **87**, 107001 (2001).
[8] H. Kawano-Furukawa, H. Takeshita, M. Ochiai, T. Nagata, H. Yoshizawa, N. Furukawa, H. Takeya, and K. Kadowaki, Phys. Rev. B **65**, 180508 (2002).
[9] P.L. Gammel, B. Barber, D. Lopez, A.P. Ramirez, D.J. Bishop, S.L. Bud'ko, and P.C. Canfield, Phys. Rev. Lett. **84**, 2497 (2000).
[10] H. Bluhm, S.E. Sebastian, J.W. Guikema, I.R. Fisher, and K.A. Moler, Phys. Rev. B **73**, 014514 (2006).
[11] S.S. James, C.D. Dewhurst, S.B. Field, D.M. Paul, Y. Paltiel, H. Shtrikman, E. Zeldov, and A.M. Campbell, Phys. Rev. B **64**, 092512 (2001).
[12] U. Yaron, P.L. Gammel, A.P. Ramirez, D.A. Huse, D.J. Bishop, A.I. Goldman, C. Stassis, P.C. Canfield, K. Mortensen, and M.R. Eskildsen, Nature (London) **382**, 236 (1996).
[13] J. Appel, *Polarons, Solid State Physics*, edited by F. Seitz and D. Turnbull (Academic, New York, 1968), Vol. 21, p. 193.
[14] T.K. Ng and C.M. Varma, Phys. Rev. Lett. **78**, 3745 (1997).
[15] T.V. Ramakrishnan and C.M. Varma, Phys. Rev. B **24**, 137 (1981).
[16] A. Shekhter, L.N. Bulaevskii, and C.D. Batista, Phys. Rev. Lett. **106**, 037001 (2011).
[17] L. Bányai, Phys. Rev. Lett. **70**, 1674 (1993).
[18] A. Hed and P. Freud, J. Non-Cryst. Solids **2**, 484 (1970).
[19] C.D. Dewhurst, R.A. Doyle, E. Zeldov, and D. McK. Paul, Phys. Rev. Lett. **82**, 827 (1999).
[20] R.J. Cava, H. Takagi, H.W. Zandbergen, J.J. Krajewski, W.F. Peck, T. Siegrist, B. Batlogg, R.B. v. Dover, R.J. Felder, K. Mizuhashi, J.O. Lee, H. Eisaki, and S. Uchida, Nature (London) **367**, 252 (1994).
[21] P. Bonville, J.A. Hodges, C. Vaast, E. Alleno, C. Godart, L.C. Gupta, Z. Hossain, R. Nagarajan, G. Hilscher, and H. Michor, Z. Phys. B **101**, 511 (1996).
[22] I.S. Veschunov, L.Y. Vinnikov, S.L. Budko, and P.C. Canfield, Phys. Rev. B **76**, 174506 (2007).
[23] P. Allenspach, B.W. Lee, D.A. Gajewski, V.B. Barbeta, M.B. Maple, G. Nieva, S.I. Yoo, M.J. Kramer, R.W. McCallum, and L. Ben-Dor, Z. Phys. B **96**, 455 (1995).